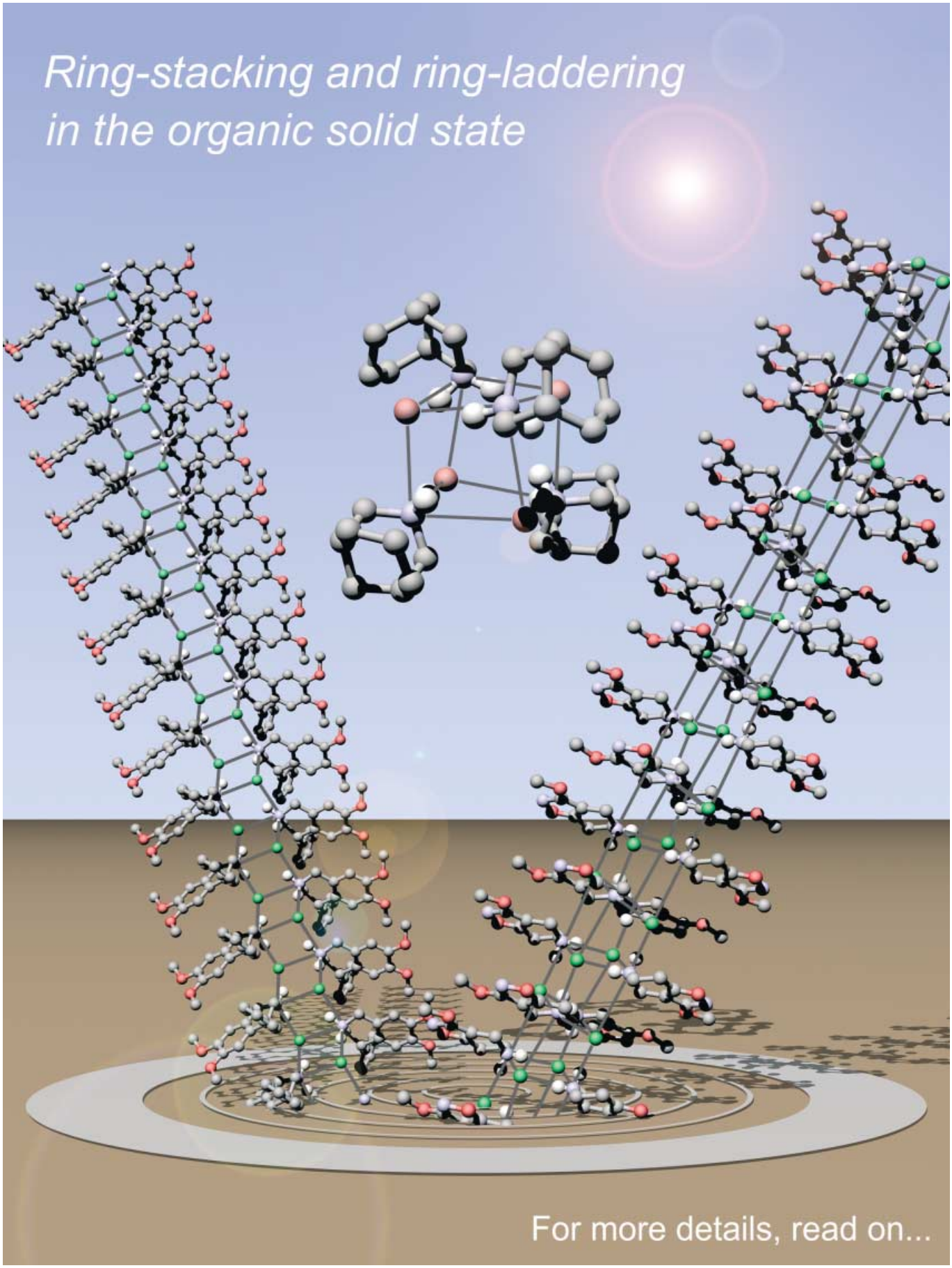

 DOI: 10.1002/chem.200305700

Structural Motifs in Secondary Ammonium Halides: Ring-Stacking and Ring-Laddering in the Organic Solid State

Andrew D. Bond*[a]

Abstract: The ring-stacking and ring-laddering concepts of structural inorganic chemistry may be applied to rationalize motifs observed for secondary ammonium halides R_2NH_2X (X = Cl, Br) in the organic solid state. General examination of the directional preferences of $N^+\cdots X^-$ contacts in 166 crystal structures confirms that the shortest contacts (3.0–3.2 and 3.2–3.4 Å, X = Cl, Br) are $N^+-H\cdots X^-$ hydrogen bonds lying approximately along the directions of the N^+-H bond vectors. The next shortest $N^+\cdots X^-$ contacts display two preferred directions of approach: i) contacts in the distance range 3.2–3.5 (X = Cl) and 3.2–3.9 Å (X = Br) lie close to the $H-N^+-H$ plane, along the direction of the bisector of the $H-N^+-H$ angle; ii) contacts in the distance range 4.0–4.2 (X = Cl) and 4.0–4.4 Å (X = Br) lie close to the $H-N^+-H$ plane, along the direction of an axis extending to the rear of one of the N^+-H bonds. Both directions of approach lead frequently to association of $R_2NH_2^+X^-$ ion pairs into laddered motifs. Stacking association is also observed, giving rise in one case to discrete cubanes and in several other cases to extended stacked-cube arrangements. In each case, the distribution of $N^+\cdots X^-$ contacts reflects a balance between the directional properties of the $N^+-H\cdots X^-$ hydrogen bonds and (primarily steric) interactions between the R groups of the organic moieties. The ladder and stack motifs of the organic ammonium halides are in many cases directly comparable to those in alkali metal amides, $[R_2NM]_n$, and information derived from the extensive organic sample provides insight into the motifs adopted by the inorganic complexes.

Keywords: database searching · halides · hydrogen bonds · ring-stacking/ring-laddering · solid-state structures

Introduction

The concepts of ring-stacking and ring-laddering, developed by Snaith and co-workers initially for alkali metal complexes,[1] find wide applicability in structural inorganic chemistry.[2] Thus, discrete M^+X^- ion pairs are envisaged to form dimeric or trimeric rings, which may associate in either a stacking manner to form tetrameric cubanes (e.g. $[Me_3Si-C_6H_8-(t\text{Bu})C{=}NLi]_4$)[3] or hexamers (e.g. $[Ph(t\text{Bu})C{=}NLi]_6$),[4] or in a lateral manner to form oligomeric (e.g. $\{[H_2C(CH_2)_3NLi]_2\cdot TMEDA\}_2$)[5] or polymeric ladders (e.g. $\{[(t\text{Bu})N(H)Na]_3\cdot(t\text{Bu})NH_2\}_8$).[6] Association is driven primarily by electrostatic forces, leading to higher coordination numbers for both M^+ and X^-, thereby maximizing Coulombic energy. The tendency towards association in either a stacking or laddering manner is sterically driven and dependent on the nature of the groups comprising the anionic moiety: where X^- contains flat groups that lie largely in the plane of the dimeric or trimeric rings, stacking is encouraged, for example, lithium imides, $[(R_2C{=}N)Li]_n$; where the R groups project above and below the dimer plane, laddering is commonly observed, for example, lithium amides, $[R_2NLi]_n$. In many cases, the R groups in the anionic moiety hinder both stacking and laddering, so that discrete dimers or trimers are found, for example, $[(2,6\text{-}(i\text{Pr})_2C_6H_3)(Me_3Si)NLi]_2$ and $[(PhCH_2)_2NLi]_3$.[7,8] The laddered, stacked, and discrete structural motifs may be viewed as successively smaller fragments of infinite $[M^+X^-]_\infty$ lattices, prevented from further association by the steric constraints of the organic moieties. In addition to a certain predictive capability, a significant strength of the ring-stacking and ring-laddering concepts is an ability to rationalize bond distances in complexes such as the alkali metal imides and amides in terms of two-center or three-center interactions, depending on whether the orbitals on N (considered as sp^2 hybrid atomic orbitals in the imides or sp^3 hybrids in the amides) are oriented directly towards one M^+ cation or point between two M^+ cations (Scheme 1).[2a]

[a] Dr A. D. Bond
University of Southern Denmark, Department of Chemistry
Campusvej 55, 5230 Odense M (Denmark)
Fax: (+45) 6615-8780
E-mail: adb@chem.sdu.dk

Supporting information for this article is available on the WWW under http://www.chemeurj.org/ or from the author. Two-dimesional chemical diagrams of all organic salts mentioned in the text are provided together with full lists of CSD refcodes and geometrical parameters for the structures included in the statistical analyses.

DOI: 10.1002/chem.200305700

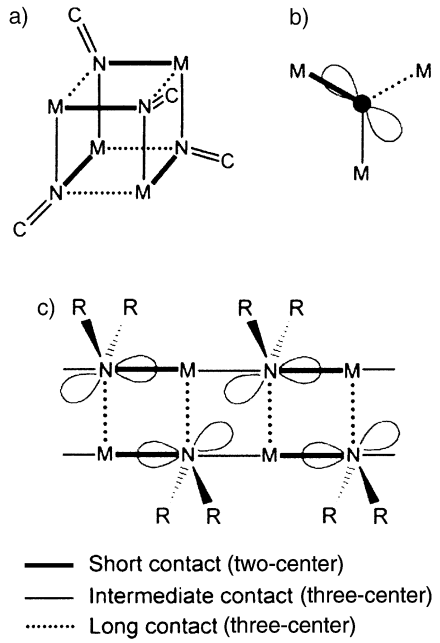

Scheme 1. Distribution of M–N distances in a) ring-stacked alkali metal imides, with b) projection along the C=N bond of the imide anion showing the orientation of sp^2 hybrid atomic orbitals on N, and c) ring-laddered alkali metal amides with sp^3 hybrid atomic orbitals depicted on N [adapted from ref. [2b]].

Organic ammonium halides, R_2NH_2X (X = halogen), fall within the traditional domain of the organic solid state, in which structures are most commonly described in terms of hydrogen-bond motifs and rationalized according to the ubiquitous supramolecular-synthon approach.[9] They are, however, inherently ionic solids, and the concepts of structural inorganic chemistry might therefore be fruitfully applied to describe their structures. An analogy between organic ammonium halides and inorganic amide complexes was suggested initially by the crystal structure of the hydrochloride of the primary amine, 2,6-di(*i*Pr)aniline,[10] in which discrete hydrogen-bonded supramolecular cubanes are observed. Analogous cubanes with comparable geometric features are formed by the complexes of Sn^{2+} and Pb^{2+} with the dianion derived from the same organic moiety.[11] From this it can be inferred that the directional bonding requirements of the three N^+–H groups of the primary ammonium moiety resemble those of three sp^3 hybrid atomic orbitals on the organic dianion, so that the directional forces responsible for self-assembly are similar in both the metal complex and the hydrogen-bonded system.[10] In this report, it is demonstrated that the analogy also encompasses secondary ammonium halides, R_2NH_2X, and alkali metal amide complexes, $[R_2NM]_n$, in which the directional bonding requirements of the two N^+–H groups of the ammonium moiety resemble those of two sp^3 hybrid atomic orbitals on the organic anion R_2N^-. In the course of this comparison, the concepts of ring-stacking and ring-laddering are naturally extended to the organic solid state.

Results and Discussion

Structural motifs in secondary ammonium halides, R_2NH_2X: The crystal structures of 166 secondary ammonium halides (148 chlorides, 16 bromides, and 2 iodides) were identified in the Cambridge Structural Database (CSD)[12] in which the N^+–H···X^- hydrogen-bond motifs are not disrupted significantly by additional hydrogen-bonding interactions (see Experimental Section).[13] The hydrogen-bond motifs comprise predominantly dimers (34 structures) and polymeric ribbons (130 structures). One example of a cyclic tetrameric motif also exists in the hydrochloride of triacetone amine.[14] The point of interest for this study is not the hydrogen-bond motifs as such, but rather the general manner in which $R_2NH_2^+X^-$ ion pairs are associated, that is, the directionality of all N^+···X^- contacts, both hydrogen-bonded and non-hydrogen-bonded, with respect to the ammonium moiety. To examine this directionality in a general sense, the three shortest N^+···X^- contacts (regardless of magnitude) were considered in each structure. Distance cut-offs were not applied at this stage to reflect the long-range nature of electrostatic forces and to ensure that the inherent directionality of the N^+···X^- contacts was not obscured. The geometry of the contacts was described according to a reference frame employed previously by Rosenfield et al. for examination of non-bonded atomic contacts to divalent sulfur:[15] the C–N^+–C unit of the secondary ammonium moiety defines a plane, and the directions of the N^+···X^- contacts are described by spherical polar coordinates, in which the azimuthal angle ϕ is the in-plane angle between the bisector of the C–N^+–C bond and the projection of the N^+···X^- vector, and the polar angle θ is the angle between the normal to the plane and the N^+···X^- vector (Figure 1). In this description,

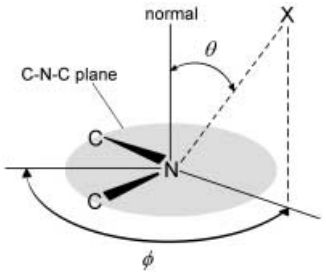

Figure 1. Spherical polar coordinate description of the directionality of the N^+···X^- contacts. The azimuthal angle ϕ is measured from the bisector of the C–N^+–C bond and the polar angle θ is measured from the normal to the C–N^+–C plane.

the N^+–H bond vectors of the ammonium moiety lie at $\phi = 180°$, $\theta \approx \pm 35°$ and the N^+–C bond vectors lie at $\phi \approx \pm 55°$, $\theta = 90$. Throughout the subsequent discussion, ϕ and θ are given as absolute values in the ranges $0 < \phi < 180°$ and $0 < \theta < 90°$ so that no distinction is made between approaches from opposite sides of the H–N^+–H or C–N^+–C planes.

Figure 2a shows scatterplots of the ϕ and θ parameters for all identified N^+···X^- vectors up to the longest observed separation (ca. 8.6 Å). The two shortest N^+···X^- contacts in

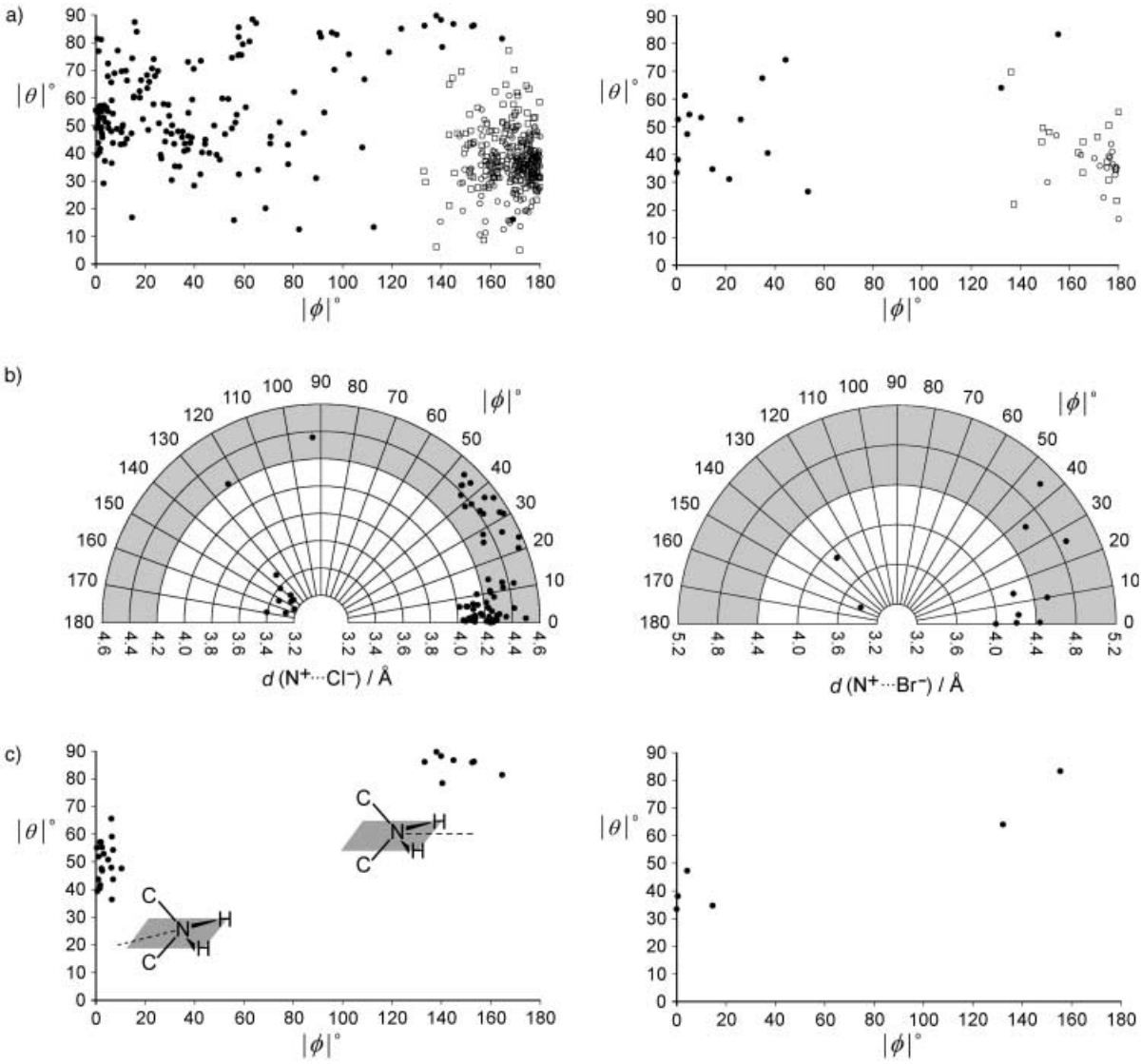

Figure 2. Distributions of the three shortest $N^+\cdots X^-$ contacts in the crystal structures of secondary ammonium chlorides (left) and bromides (right): a) all identified contacts (up to the longest of ca. 8.6 Å), with the shortest contact in each structure denoted by an open circle, the intermediate contact by an open square, and the longest contact by a filled circle; b) polar plot of the ϕ parameter versus the $N^+\cdots X^-$ separation; the shaded region denotes broadening of the directionality and sets the distance cut-off for subsequent discussion; c) third-longest contacts only with $N^+\cdots X^-$ less than 4.2 Å for Cl and 4.4 Å for Br.

each case correspond to hydrogen-bond interactions and are clustered around $\phi = 180°$, $\theta \approx 35°$, the directions of the N^+–H bond vectors. It is the next shortest contacts that are of greatest interest. Figure 2b shows polar plots of the ϕ parameter versus the magnitude of the $N^+\cdots X^-$ vector for the third longest contact in each structure. Considering initially the chlorides, it is clear that the shortest contacts display distinct clustering around two regions: ϕ = 130–170° and ϕ = 0–10°. The first region contains the shortest contacts of all (3.2–3.5 Å), while the second contains somewhat longer contacts (4.0 Å and above). As the $N^+\cdots Cl^-$ distance increases above about 4.2–4.3 Å, the distribution broadens and the directional preferences of the contacts become more diffuse. The subsequent discussion is focussed therefore predominantly on structures with $N^+\cdots Cl^-$ contacts below 4.2 Å; application of the distance cut-off at this stage is made on the basis of the observed *directionality* of the contacts rather than any arbitrary distance criterion. For the bromides, of which there are far fewer examples, clustering is necessarily less distinct but the distribution resembles that of the chlorides: the shortest $N^+\cdots Br^-$ contacts (3.2–3.9 Å) lie in the region ϕ = 130–170°, and the next shortest (4.0–4.4 Å) lie in the region ϕ = 0–10°. Broadening of the distribution in this case is observed above an $N^+\cdots Br^-$ distance of about 4.4 Å and this cut-off is applied for subsequent discussion. For the iodides, there are too few structures for meaningful discussion and these are not considered further.

Figure 2c displays scatterplots of the ϕ and θ parameters for only those third-longest $N^+\cdots X^-$ vectors with magnitude less than the specified distance cut-offs. For the chlorides, the contacts are clearly clustered into two regions: ϕ = 130–170°, θ = 80–90° (Region 1) and ϕ = 0–10°, θ = 35–

65° (Region 2). For the bromides the clustering is less distinct but again resembles that of the chlorides. The first region corresponds to approach of X^- in the plane of the NH_2^+ group approximately along the bisector of the H–N^+–H angle, that is, towards the midpoint of the H···H edge of the pseudo-tetrahedral $R_2NH_2^+$ unit. This direction of approach is the least sterically hindered and gives rise to the shortest $N^+\cdots X^-$ contacts. The second region also corresponds to approach of X^- in the plane of the NH_2^+ group, but in this case along an axis to the rear of one N^+–H bond, that is, towards the center of one R_2H face of the pseudo-tetrahedral $R_2NH_2^+$ unit. The longer $N^+\cdots X^-$ contacts observed in this region are consistent with a more hindered approach resulting from the steric bulk of the R groups. The structures populating the two regions are discussed in turn.

Region 1: ϕ = 130–170°, θ = 80–90°: Eleven structures (9 chlorides, 2 bromides) were identified within the specified distance limits in which the third $N^+\cdots X^-$ contact lies in the region ϕ = 130–170°, θ = 80–90° (Table 1). In nine of these, lateral association leads to formation of extended polymeric ladders, hereafter referred to as Type 1 (Figure 3). In each case (except for the symmetric VABFIN), the ladder conformation is fully *transoid*, that is, at each subsequent organic moiety along the ladder, equivalent R groups lie on opposite sides of the plane containing the N^+(–H)···X^- contacts. The magnitudes of the three $N^+\cdots X^-$ contacts that define the motif are comparable within each structure and lie in the range 3.0–3.4 Å. In all but one case (the exception being CETEAN10), the distribution of $N^+\cdots X^-$ distances is identical to that in archetypal ring-laddered lithium amides: short and intermediate distances alternate along the ladder arms, while significantly longer contacts comprise the ladder rungs (Figure 3).[2a] Thus, secondary ammonium halides forming Type 1 ladders display ring-laddering behavior *exactly* analogous to that of alkali metal amides. In the same way that the distribution of M–N distances in the lithium amides may be considered to reflect the formation of two-center and three-center interactions involving sp^3 hybrid atomic orbitals on N (Scheme 1), so the $N^+\cdots X^-$ distances in the ammonium halides reflect the formation of non-bifurcated and bifurcated hydrogen bonds (Figure 3). In general, one short non-bifurcated (two-center) interaction and two longer bifurcated (three-center) interactions are formed by each ammonium center. The non-bifurcated $N^+\cdots X^-$ contacts are comparable in magnitude to those in isolated tertiary ammonium halides, R_3NHX: average $N^+\cdots Cl^-$ 3.07(7) Å, $N^+\cdots Br^-$ 3.25(7) Å.[17] The relative magnitudes of the longer $N^+\cdots X^-$ contacts reflect primarily the associated N^+–H···X^- angles: the $N^+\cdots X^-$ distance is inversely correlated with the N^+–H···X^- angle in the manner typical of strong hydrogen bonds.[18] The concept of the two-center and three-center interactions is perhaps illustrated rather more clearly in the hydrogen-bonded systems than in the inorganic systems, since the N^+–H bond vectors in the former are readily apparent—these effectively "map" the implied orientations of sp^3 hybrid atomic orbitals in the inorganic systems.

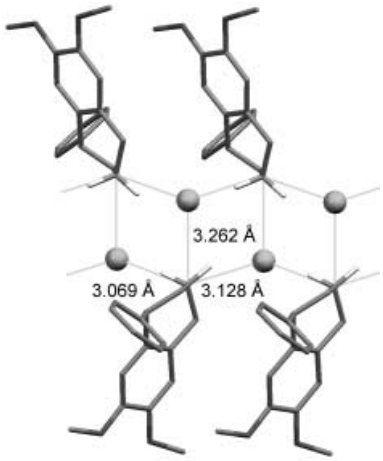

Figure 3. Hydrogen-bonded ladder (Type 1) in the crystal structure of PEFCUY. Hydrogen atoms not involved in hydrogen bonding are omitted.

The organic moieties that form Type 1 ladders display several comparable features: in all but one of the chlorides, the NH_2^+ center forms part of a piperidinium or pyrrolidinium ring, so that the bulk of each organic moiety lies to the outside of the ladder arms. The majority of ring-laddered lithi-

Table 1. Secondary ammonium halides forming three short $N^+\cdots X^-$ contacts, in which the third $N^+\cdots X^-$ contact (< 4.2, 4.4 Å for X = Cl, Br) lies in Region 1 (ϕ = 130–170°, θ = 80–90°).[a]

		d [Å]	ϕ [°]	θ [°]	d [Å]	ϕ [°]	θ [°]	d [Å]	ϕ [°]	θ [°]
Ring-laddering			Ladder arm 1			Ladder arm 2			Ladder rung	
BORXUB	Cl	3.094	171.0	18.9	3.143	178.6	26.5	3.346	152.5	85.9
BRPYRL	Cl	3.009	174.5	19.4	3.289	132.9	33.5	3.300	138.0	89.7
CETEAN10	Cl	3.155	149.3	39.8	3.404	169.1	16.1	3.169	175.5	63.2
HOTZOF	Cl	3.066	172.0	13.6	3.124	161.1	31.6	3.389	139.9	88.2
PEFCUY	Cl	3.069	175.3	31.4	3.127	133.6	29.6	3.262	140.4	78.4
SIFGUJ	Cl	3.075	148.7	19.2	3.112	151.5	33.2	3.268	144.9	86.7
SOBFIY	Cl	3.048	179.1	26.0	3.093	157.2	8.6	3.267	164.6	81.4
TAJRUR	Br	3.273	151.1	30.0	3.373	137.3	22.0	3.400	155.4	83.3
VABFIN	Cl	3.032	167.1	15.6	3.095	170.0	25.5	3.220	153.2	86.2
Ring-stacking										
AZNONB	Br	3.193	173.9	24.4	3.496	136.2	69.7	3.898	132.2	64.0
ZENJAD	Cl	3.096	166.8	34.3	3.124	143.1	46.7	3.479	133.2	86.1
		4.240	44.8	33.2						

[a] Literature references given in ref. [16].

um amide complexes are also derived from cyclic organic moieties, including the piperidide[19] and pyrrolidide anions.[5] In most of the organic structures, the piperidinium or pyrrolidinium groups bear only flat ring-based substituents that stack in a face-to-face manner along the ladder arms. The distribution of $N^+\cdots X^-$ distances is clearly influenced by interactions between adjacent organic moieties: in BORXUB, for example, the short and intermediate contacts along the ladder arms (3.094 and 3.143 Å) are not correlated with the $N^+-H\cdots Cl^-$ angles (169.4 and 157.8°, respectively) in the expected manner. Thus, the $N^+\cdots X^-$ distance distribution is shown to be a balance between the directional preferences of the hydrogen bonds and interactions between the R groups of the organic moieties. In addition to an influence on the magnitude of the $N^+\cdots X^-$ contacts, optimization of the interactions between organic moieties is manifested in differing degrees of rotation of the $H-N^+-H$ bisector (i.e. the $C-N^+-C$ plane) from the direction of the ladder rungs. This is reflected statistically in a widening of the $N^+\cdots X^-$ contact distribution in ϕ (Figure 2c).

In the chloride CETEAN10 (Figure 4) and the bromide TAJRUR, the NH_2^+ center forms part of a noncyclic organic moiety. In CETEAN10, all of the $N^+\cdots Cl^-$ contacts are

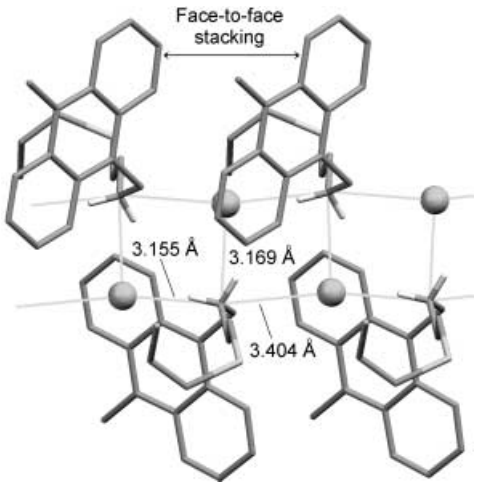

Figure 4. Type 1 ladder motif in CETEAN10. Hydrogen atoms not involved in hydrogen bonding are omitted. The R groups of the noncyclic organic moiety lie to a greater degree above and below the ladder plane compared with the ladders based on cyclic organic moieties (e.g. Figure 3). The distribution of $N^+\cdots X^-$ distances is clearly influenced by face-to-face stacking between adjacent anthracene groups.

significantly longer than those in the other chlorides described thus far and the distances are distributed differently: an intermediate contact makes up the ladder rung, while short and long contacts alternate along the ladder arms.[20] This may be attributed to steric constraints imposed by interactions between the organic moieties extending above and below the plane of the ladder motif; although the $N^+\cdots Cl^-$ contacts in CETEAN10 are longer than those in the other Type 1 ladders, the cross-ladder separation between the α-C atoms is considerably shorter (ca. 5.00 Å compared with 6.14–6.60 Å in the other chlorides). One particularly long $N^+\cdots Cl^-$ contact within the ladder arm of CETEAN10 (3.404 Å) is also clearly influenced by face-to-face stacking of adjacent anthracene groups. In TAJRUR, the $N^+\cdots Br^-$ contacts are significantly longer than the $N^+\cdots Cl^-$ contacts in CETEAN10 and the $N^+\cdots Br^-$ distance distribution is comparable to that observed in the other Type 1 ladders.

In the two remaining examples within Region 1, AZNONB and ZENJAD, the third $N^+\cdots X^-$ contacts lie towards the edges of the distribution, both in their magnitude and in the angle ϕ (Table 1). In both cases, the intermediate $N^+\cdots X^-$ contacts also lie at the edges of the expected ranges. Examination of these structures reveals that association occurs in a stacking manner. The bromide AZNONB forms discrete cubanes in which the distribution of $N^+\cdots Br^-$ distances is entirely consistent with that predicted by the ring-stacking concept: four short and four long *intra*-dimer distances, with four intermediate *inter*-dimer distances considered to define the ring-stacking direction (Figure 5a).[2a]

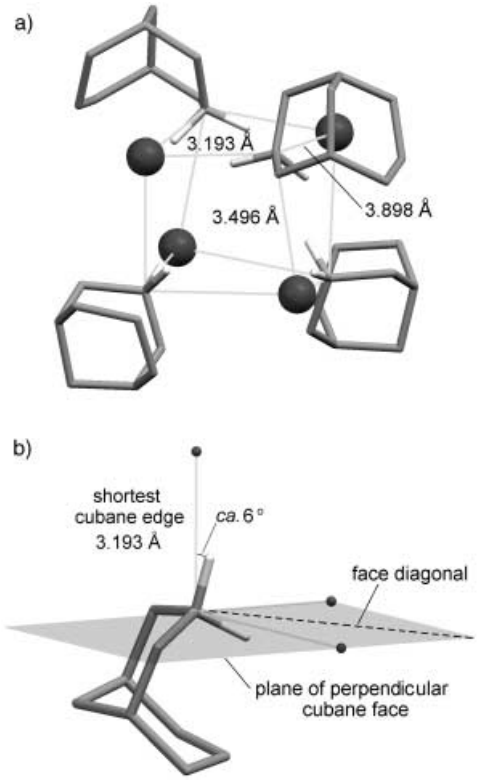

Figure 5. a) Ring-stacked cubane unit in AZNONB. Hydrogen atoms bound to carbon are omitted. The orientation of the cubane and the $N^+\cdots Br^-$ distance distribution corresponds to that shown in Scheme 1. b) Orientation of the $C-N^+-C$ plane with respect to the shortest cubane edge.

As observed for the ladders, each ammonium center adopts one short interaction that coincides closely with one N^+-H bond vector and one intermediate and one long interaction that comprise a bifurcated hydrogen bond. The $C-N^+-C$ plane of the organic moiety lies close to perpendicular to the shortest cube edge, tilted slightly from it to bring one N^+-H bond close to parallel to that edge (Figure 5b); a similar arrangement is observed in the hydrogen-bonded cubane of 2,6-di(*i*Pr)aniline hydrochloride.[10] The other N^+

−H bond in AZNONB points almost directly across the diagonal of the perpendicular cube face so that the two N^+−H···Br^- angles are approximately equal. The considerable difference in magnitude of the associated N^+···Br^- contacts therefore is not a simple reflection of the deviation from linearity of the hydrogen-bond interactions, but again is shown to reflect a balance between the directional properties of the hydrogen bonds and the steric constraints imposed by the organic moieties. The observation of discrete ring-stacked cubanes incorporating secondary *ammonium* moieties is perhaps unexpected since the steric constraints imposed by secondary amido anions generally prevent stacking in inorganic systems. The metric features of the cube edges are clearly significant: typical N···Li distances in lithium amides lie in the range 2.0–2.2 Å and ring-stacking is not observed in these systems. The N^+···Br^- distances in AZNONB (ca. 3.2 Å and higher) are significantly longer, relaxing the steric constraints and permitting ring-stacking.

The final structure within Region 1, ZENJAD, displays slightly different behavior: each NH_2^+ center adopts one short, one intermediate, and one long N^+···Cl^- contact, comparable to the situation in AZNONB, but association occurs to form an extended stacked-cube arrangement that includes a fourth short N^+···Cl^- contact of 4.240 Å. Discussion of this extended motif is deferred for convenient comparison with several other higher-order structural motifs.

Region 2: ϕ = 0–10°, θ = 35–65°: Sixteen structures (14 chlorides, 2 bromides) were identified within the specified distance limits in which the third N^+···X^- contact lies in the region ϕ = 0–10°, θ = 35–65° (Table 2). In each of these cases, lateral association gives rise to polymeric ladders with fully *transoid* conformations, but the distribution of N^+···X^- contacts is distinctly different from that of the previous examples: two short contacts of comparable magnitude (ca. 3.0–3.3 Å) comprise the ladder rung and one section of the ladder arm, while a third significantly longer contact (ca. 4.0–4.3 Å) forms the second section of the ladder arm (as, for example, in Figure 6). These ladders are hereafter referred to as Type 2. In all cases, the shorter contacts in one ladder arm lie opposite the longer ones in the other arm so that there is no clear distinction between hydrogen-bonded dimeric units and *inter*-dimer N^+···X^- contacts. Thus, the concept of ring-laddering within these systems does not necessarily imply lateral association of *hydrogen-bonded* dimers, but rather lateral association of $[R_2NH_2^+X^-]_2$ units. The hydrogen-bond motif within these ladders in fact resembles a *trans–trans* ribbon, in which each NH_2^+ center forms two non-bifurcated (two-center) hydrogen bonds, and a third essentially electrostatic (non-hydrogen-bonded) con-

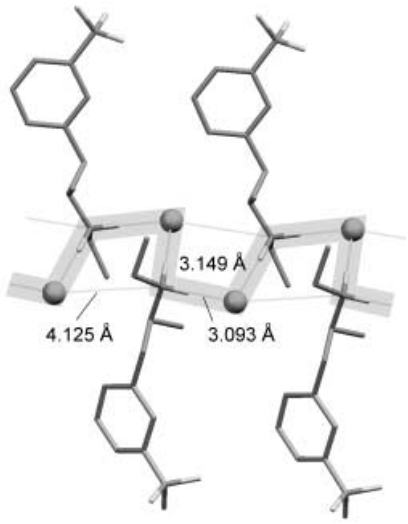

Figure 6. Type 2 ladder structure in BUHCIQ. Hydrogen atoms not involved in hydrogen bonding are omitted. Each ammonium center forms two non-bifurcated (two-center) hydrogen bonds and one longer electrostatic contact. The *trans–trans* hydrogen-bonded ribbon motif is shaded.

Table 2. Secondary ammonium halides forming three short N^+···X^- contacts, in which the third N^+···X^- contact (< 4.2, 4.4 Å for X = Cl, Br) lies in Region 2 (ϕ = 0–10°, θ = 35–65°).[a]

		d [Å]	ϕ [°]	θ [°]	d [Å]	ϕ [°]	θ [°]	d [Å]	ϕ [°]	θ [°]
Ring-laddering			Ladder arm 1			Ladder arm 2			Ladder rung	
BOTPAB	Cl	3.155	173.8	36.0	4.056	0.6	39.4	3.153	173.2	44.0
BUHCIQ	Cl	3.093	179.5	37.5	4.124	0.4	55.1	3.149	178.8	32.9
CARQIV	Br	3.299	165.5	44.6	4.208	14.6	34.7	3.290	177.0	43.8
DIZVUD	Cl	3.100	160.9	40.9	4.115	2.3	47.6	3.101	162.9	36.7
HIYDOI	Cl	3.082	177.6	34.7	4.127	2.6	46.8	3.104	170.8	39.0
JARSAW	Cl	3.164	149.9	47.2	4.089	1.8	41.6	3.077	173.7	39.8
KADNIM	Cl	3.147	176.6	37.0	4.080	1.6	40.4	3.155	174.5	42.6
MIXTAO	Cl	3.133	175.9	45.7	4.169	3.2	52.9	3.112	178.3	31.0
		3.098	175.4	47.3	4.217	7.0	54.3	3.131	176.2	28.2
POJVOZ	Br	3.326	171.4	46.3	4.224	4.3	47.3	3.242	175.3	35.2
POJVUF	Cl	3.087	169.7	48.3	4.120	7.0	43.7	3.098	177.8	34.9
SIWCAC	Cl	3.227	167.3	77.2	4.067	6.3	65.6	3.052	139.7	15.3
VIPNIR	Cl	3.116	155.9	48.9	4.041	1.0	43.7	3.123	166.5	36.0
WOGPOX	Cl	3.128	169.6	34.6	4.156	10.4	47.6	3.128	149.7	41.7
WOWXIP[b]	Cl	3.090	176.6	38.2	4.127	2.1	57.1	3.144	180.0	31.3
WOWXUB[b]	Cl	3.091	177.0	38.2	4.130	1.7	57.1	3.145	179.7	31.4
YIJFOM	Cl	3.223	165.8	47.4	4.076	6.3	47.9	3.101	161.9	34.9
		3.178	169.1	49.4	4.118	5.0	50.8	3.083	163.7	31.1

[a] Literature references given in ref. [21]. [b] Stereoisomers.

tact (Figure 6). The ladders are polar (i.e. all N–H bonds within both ladder arms point in the same direction) and in most cases are formed along crystallographic 2_1 screw axes. As observed for the Type 1 ladders, the H–N^+–H bisector displays a range of rotation with respect to the ladder rungs, in this case giving rise to a widening of the angle θ in the $N^+\cdots X^-$ distribution (Figure 2c).

Among the Type 2 ladders, there is a considerably greater proportion of noncyclic ammonium moieties. As described previously for CETEAN10, the R groups of noncyclic moieties project to a greater degree above and below the ladder plane compared with their cyclic counterparts, increasing the significance of steric repulsions between them and giving rise to elongation of the $N^+\cdots X^-$ contacts in Type 1 ladders. The increased proportion of noncyclic ammonium moieties populating Region 2 suggests that as the steric constraints associated with the formation of Type 1 ladders become more severe, Type 2 ladders become more prevalent.

There are also four Type 2 ladders based on cyclic ammonium moieties (DIZVUD, HIYDOI, JARSAW, POJVOZ) bearing flat ring-based substituents, similar to those shown previously to form Type 1 ladders. The structure of HIYDOI in particular resembles closely that of CETEAN10 in the manner in which ring-based substituents are stacked along the ladder arms (Figure 7). The distinction between

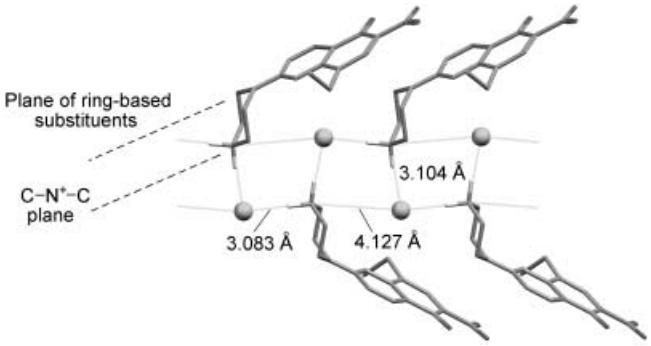

Figure 7. Type 2 ladder in HIYDOI. Hydrogen atoms not involved in hydrogen bonding are omitted. The planes of the ring-based substituents lie approximately parallel to the C–N^+–C planes.

the Type 2 ladder in HIYDOI and the Type 1 ladder in CETEAN10 reflects the orientation of the stacked substituents with respect to the C–N^+–C plane: the ring plane of the stacked groups lies essentially parallel to the C–N^+–C plane in HIYDOI, but close to perpendicular to the C–N^+–C plane in CETEAN10. Thus, comparable face-to-face stacking of ring-based substituents in the two cases leads to differing alignments of the C–N^+–C planes with respect to the ladder arms and therefore different distributions of $N^+\cdots X^-$ contacts. In the other three examples based on cyclic ammonium moieties (DIZVUD, JARSAW, POJVOZ), the distinction between the Type 2 and Type 1 ladders reflects the fact that the rings on adjacent organic moieties within the Type 2 ladder arms do not adopt face-to-face stacked arrangements with each other, but are interdigitated with rings from *adjacent* ladder moieties (e.g. Figure 8). This presumably reflects the preferences of the ring-based substituents to align with each other in a parallel or anti-parallel manner.

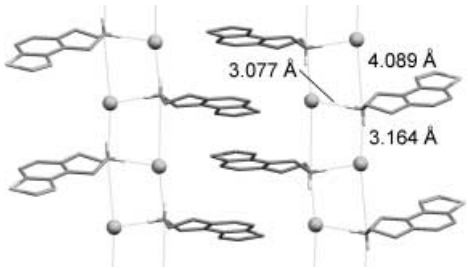

Figure 8. Interdigitation between ring-based substituents of adjacent Type 2 ladders in JARSAW. Hydrogen atoms not involved in hydrogen bonding are omitted.

In both Type 1 and Type 2 ladders, the underlying manner of association of the $R_2NH_2^+X^-$ ion pairs and the resulting spatial distribution of the N^+ and X^- centers is comparable. The distinction between the two ladder types lies in the orientation of the organic moiety with respect to the ladder motif: in the Type 1 ladders, the C–N^+–C plane lies approximately perpendicular to the ladder arms (i.e. the bisector of the H–N^+–H angle lies parallel to the ladder rungs), while in Type 2 ladders, the C–N^+–C plane lies closer to 20° to the ladder arms (i.e. one N^+–H bond lies parallel to the ladder rungs). The adoption of the Type 1 or Type 2 arrangement is driven by optimization of interactions between the R groups of the organic moieties—both within and between ladders—and the resulting distribution of $N^+\cdots X^-$ distances may be considered to be a "fine-tuning" effect dependent on this alignment. Where the orientation is such that two linear (two-center) hydrogen bonds and one predominantly electrostatic contact are formed (i.e. Type 2 ladders), the distinction between short hydrogen-bonded interactions and longer non-hydrogen-bonded $N^+\cdots X^-$ contacts is most clear. Where all three $N^+(-H)\cdots X^-$ contacts resemble two-center or bifurcated (three-center) hydrogen bonds (i.e. Type 1 ladders), all three contacts are relatively short and the distinction between them is less marked. The third longest contact in the Type 1 ladders is in every case considerably shorter than that in the Type 2 ladders since Region 1 corresponds to approach towards the midpoint of the H···H edge of the $R_2NH_2^+$ moiety, the least hindered direction. The third $N^+\cdots X^-$ contact in the Type 2 arrangement is necessarily longer since approach towards the center of one R_2H face of the pseudo-tetrahedral $R_2NH_2^+$ unit is more hindered.

Higher-order structural motifs: Several structures were identified in which there are four $N^+\cdots X^-$ contacts of comparable magnitude. For brevity, the discussion is focussed primarily on those structures for which the third longest $N^+\cdots X^-$ contact falls within the previously specified distance limits (Table 3). In all but one of these examples (the exception being the previously mentioned ZENJAD), both the third and fourth longest $N^+\cdots X^-$ contacts lie in Region 2. In five

Table 3. Selected secondary ammonium halides forming higher-order structure motifs through four short $N^+\cdots X^-$ contacts.[a]

			d [Å]	ϕ [°]	θ [°]	d [Å]	ϕ [°]	θ [°]
GEQWUU	Br	4^4 net	3.259	180	16.7	3.329	180	55.3
			3.994	0	33.4	4.340	0	67.2
JINGIW	Cl	4^4 net	3.061	174.0	29.5	3.065	177.5	39.7
			4.152	6.5	59.1	4.233	6.1	47.0
MAESCI	Cl	4^4 net	3.073	178.7	38.2	3.108	175.2	35.8
			4.018	6.5	36.4	4.321	17.3	47.6
POSTUM	Br	Type 2 associated helices	3.257	172.4	35.8	3.274	175.3	37.3
			4.200	0.5	38.1	4.325	3.2	42.6
SEFWAB	Cl	4.8^2 net	3.182	173.3	34.8	3.268	170.3	30.0
			4.179	2.5	55.2	5.448	25.9	39.9
YUWWIW[b]	Cl	4^4 net	3.091	170.9	33.1	3.109	163.1	35.7
			4.099	1.1	51.9	4.195	5.7	52.0
			3.130	163.9	33.3	3.130	163.9	33.3
			4.270	8.1	52.2	4.270	8.1	52.2

[a] Literature references given in ref. [22]. [b] Two crystallographically independent molecules, the second lying on a twofold axis.

of those six structures, lateral association occurs to give two-dimensional nets, in most cases 4^4 nets (e.g. Figure 9a).[23] These motifs may be considered to be derived from Type 2 lateral association of Type 2 ladders. In each 4^4 net, the ammonium moiety is noncyclic and the R groups project above and below the plane containing the $N^+(-H)\cdots X^-$ contacts. In three cases (GEQWUU, JINGIW, and MAESCI), the R groups comprise aromatic rings that stack in a face-to-face manner. In YUWWIW, the organic moieties are chain-like so that they present minimal steric hindrance to lateral association (Figure 9b). The structure of YUWWIW is notable since the hydrogen-bond motif may be classified uniquely as a *cis-trans* ribbon (i.e. each organic moiety lies on the same side of the ribbon as one of its neighbors, but on the opposite side from its other neighbor). Examination of all $N^+\cdots X^-$ contacts in the structure reveals clearly the formation of a 4^4 net comparable to those in GEQWUU, JINGIW, and MAESCI; the unique hydrogen-bond motif in YUWWIW arises simply as a result of the arrangement of the organic moieties within this two-dimensional framework, influenced by interactions between the R groups within and between nets. In SEFWAB, one $N^+\cdots X^-$ contact from each N^+ center is particularly long (5.448 Å), giving rise to an apparent 4.8^2 net rather than a 4^4 net. This may be attributed simply to the presence of one particularly bulky R group, which projects along the direction of the elongated $N^+\cdots X^-$ vector (Figure 9c).

The structure of the sixth example within the group, dimethylammonium bromide (POSTUM), is relatively more complex. The two shortest $N^+\cdots Br^-$ contacts (3.257 and 3.273 Å) comprise non-bifurcated hydrogen bonds, which link the molecules into helices along crystallographic 2_1 screw axes (Figure 10). The next two shortest contacts (4.200 and 4.325 Å) between helices are archetypal Region 2 contacts, so that the structure may be described in terms of Type 2 association of hydrogen-bonded helices. The resemblance between this structure and the helical solid-state structure of lithium diisopropylamide $[(i\mathrm{Pr}_2\mathrm{NLi})_\infty]$ is noteworthy.[24]

Among the group of higher-order structural motifs, the previously mentioned chloride ZENJAD is unique since it is the only example in which the third longest $N^+\cdots X^-$ contact

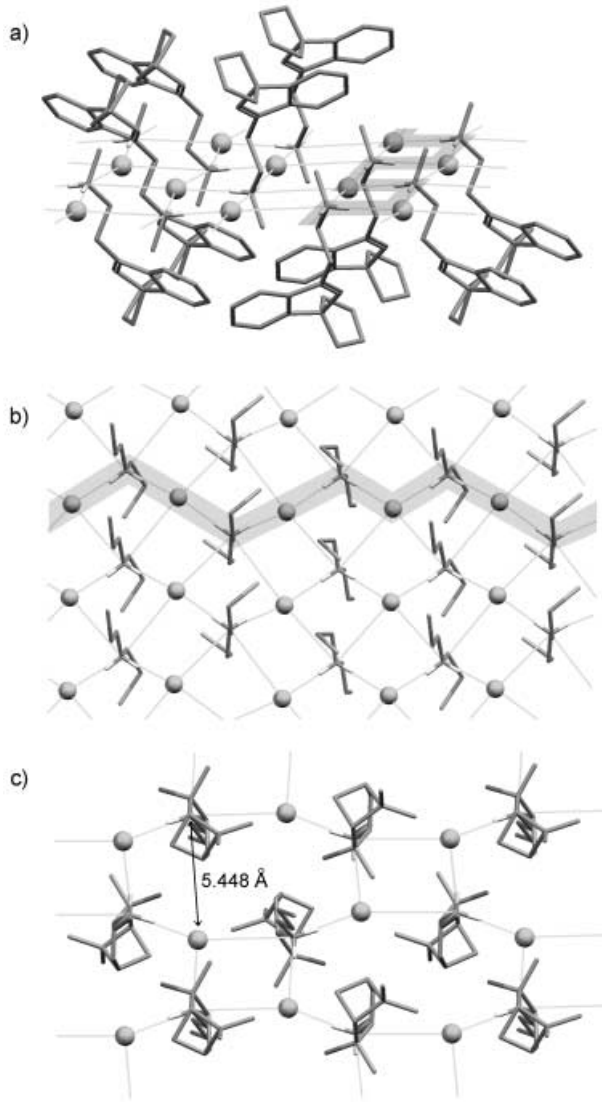

Figure 9. a) 4^4 net in MAESCI exhibiting a *trans-trans* hydrogen-bond motif (shaded); b) projection onto the plane of the 4^4 net in YUWWIW exhibiting a unique *cis–trans* hydrogen-bond motif (shaded); c) projection onto the plane of the 4.8^2 net in SEFWAB derived from elongation of one $N^+\cdots X^-$ contact parallel to the direction of projection of the bulky R group. In each figure, H atoms not involved in hydrogen bonding are omitted.

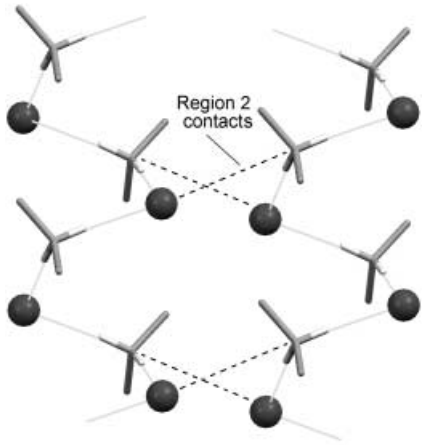

Figure 10. Hydrogen-bonded helices in POSTUM, showing Region 2 contacts between them. Hydrogen atoms not involved in hydrogen bonding are omitted.

lies within Region 1. The structure may be considered either as $[R_2NH_2^+X^-]_2$ units associated in a stacking manner along the extended axis or as two Type 2 ladders associated in a stacking manner (Figure 11). On the basis of the observed

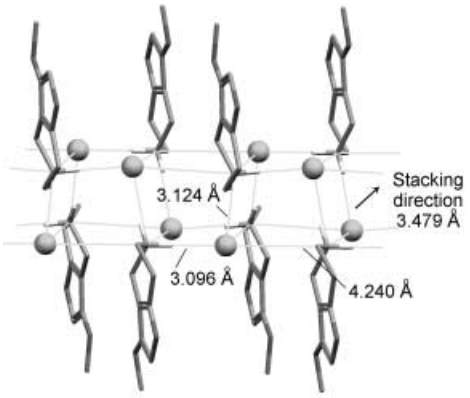

Figure 11. Extended stacked-cube motif in ZENJAD. The motif may be considered to comprise Type 2 ladders (parallel to the plane of the page) stacked through Region 1 contacts. H atoms not involved in hydrogen bonding are omitted.

$N^+\cdots Cl^-$ distance distribution, the latter description is probably most appropriate: two Type 2 ladder motifs may be envisaged, comprising two short non-bifurcated hydrogen bonds and one considerably longer Region 2 contact, in this case the *fourth* longest $N^+\cdots X^-$ contact. Interdigitation between ring-based substituents on adjacent ladders is observed, comparable to that in DIZVUD, JARSAW, and POJVOZ (Figure 8). The Type 2 ladders may then be considered to be stacked via the Region 1 contacts, which comprise all of the contacts perpendicular to the ladder planes. Description of the "stacking direction" in this manner is most consistent with that defined in AZNONB. The distinction between the two possible descriptions of the motif is perhaps not entirely arbitrary: in the first description, association is considered to be only of a stacking type, while in the second description both lateral and stacking modes of association are displayed.

Further examination of the structures beyond the imposed distance cut-offs reveals numerous additional examples of comparable higher-order structural motifs. The bromide ZIVMUM, for example, in which the R groups comprise extended *n*-octadecyl chains, provides a clear example of a 4^4 net formed by association of chain-like organic moieties lying perpendicular to the plane of the $N^+(-H)\cdots X^-$ contacts.[25] Several extended motifs based on stacking association are also evident: the previously mentioned Type 2 ladder POJVUF associates to form a distorted stacked-cube arrangement similar to that in ZENJAD (Figure 12a), in

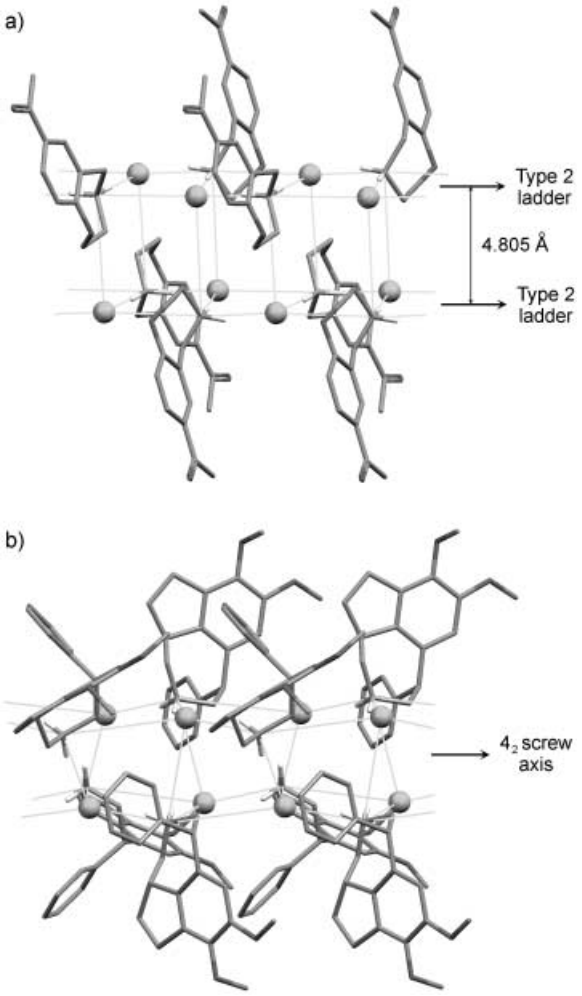

Figure 12. Extended stacked-cube motifs in a) POJVUF and b) DUTKAE10. Hydrogen atoms not involved in hydrogen bonding are omitted.

which the "*inter*-ladder" contacts are 4.805 Å ($\phi = 88.8$, $\theta = 87.5°$). A further variation of the stacked-cube motif is observed in the chloride DUTKAE10.[26] In this case, the stack is formed about a crystallographic 4_2 screw axis, with one N^+-H bond of each organic moiety pointing approximately along the extended axis (the 4_2 axis) and the other pointing along each of the four sides of the motif in turn

(Figure 12b). The fourfold symmetric arrangement of the $N^+\cdots X^-$ distances leads to a somewhat distorted motif in which it is not possible to distinguish clearly either hydrogen-bonded dimers or stacked Type 2 ladders. In this case, a description as $[R_2NH_2^+X^-]_2$ units stacked along the extended axis is probably most appropriate.

Comparison of organic and inorganic ring-laddered systems: General examination of the geometries of N–M contacts in complexes of secondary amides R_2N^- ($R \neq H$) with alkali metals reveals a somewhat larger spread in the angles ϕ and θ compared with the organic ammonium halides (Figure 13).

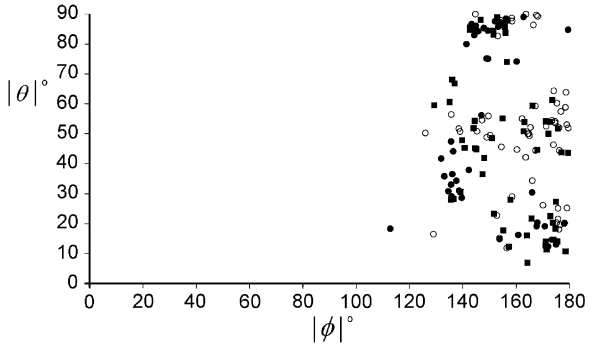

Figure 13. Distribution of the three shortest N–M contacts in complexes of secondary amido anions R_2N^- ($R \neq H$) with alkali metals. The shortest N–M contact in each structure is denoted by an open circle, the intermediate contact by a filled square, and the longest contact by a filled circle.

There is, however, one particularly notable feature of the distribution: in the metal complexes, *all* N–M contacts have $\phi > 90°$, so that they occur always from the least-hindered side of the R_2N^- moiety. Thus, all examples of inorganic amide ladders known to date are Type 1. The contacts towards the edges of the distribution (ϕ = 110–130°) are derived mostly from bidentate ligands such as ethylenediamine derivatives (e.g. $\{[(t\text{Bu})N(H)CH_2CH_2N(t\text{Bu})Li_2]_2(t\text{-Bu})NCH_2CH_2N(t\text{Bu})\}$ (TETGOO)[27]), which clearly influences the directional preferences.[28] It might also be noted that many of the ladders contain either cyclic piperidide or pyrrolidide anions and that there are no examples to date of *infinite* polymeric ladders based on R_2N^- moieties ($R \neq H$); fragmentation of the ladder motifs by Lewis base coordination (solvation) is most common.

In seeking to rationalize these observations, information derived from the far more extensive organic sample provides insight. The elongation of the $N^+\cdots X^-$ contacts in CETEAN10 together with the prevalence of noncyclic ammonium moieties among the Type 2 organic ladders suggests that the steric constraints imposed by noncyclic amide moieties hinder formation of Type 1 ladders. These steric constraints will be even more severe in inorganic complexes compared with their organic counterparts since intra-complex Li–N or Na–N interactions are considerably shorter than $N^+(-H)\cdots X^-$ contacts. Thus, alkali metal amides are unlikely to form extended Type 1 ladder motifs with noncyclic R_2N^- moieties ($R \neq H$); none have been observed to date. In the organic systems, the steric constraints associated with formation of extended Type 1 ladders lead to an increased prevalence of Type 2 ladders among noncyclic ammonium moieties. Type 2 ladders are not observed for inorganic complexes and the steric constraints are alleviated in two quite different ways. First, where Type 1 ladder formation is hindered, Lewis base coordination (solvation) and consequent ladder fragmentation appears to compete favorably. Ladder fragmentation is observed frequently in inorganic systems, even with cyclic amide moieties, reflecting the more severe steric constraints resulting from the relatively short M–N distances. Competition from solvation almost certainly accounts for the complete absence (to date) of Type 2 ladders in inorganic systems: while each M^+ cation would be forced to adopt one relatively long M–N contact in a Type 2 ladder, the formation of smaller solvated fragments allows all contacts to M^+ to be shorter, thereby maximizing Coulombic energy. An alternative means observed in the alkali metal complexes for alleviating the steric constraints is the formation of cyclized ladders (Figure 14): cyclization increases the magnitude of the "co-

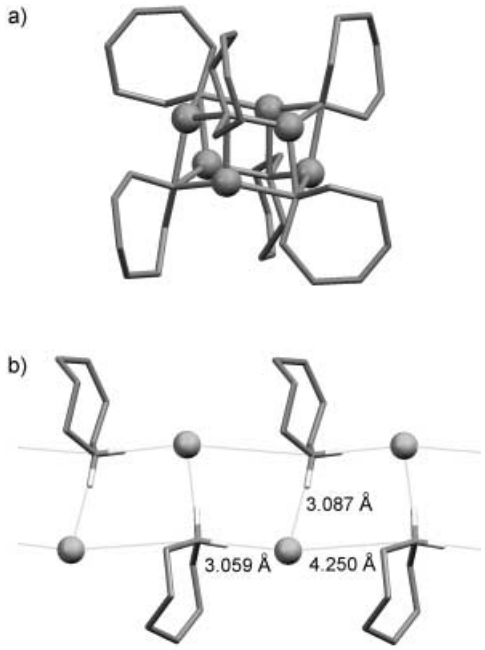

Figure 14. a) Cyclized ladder in SEDVEC; b) Type 2 ladder in HEXAMC. Both structures incorporate the hexamethyleneimine moiety. Hydrogen atoms not involved in hydrogen bonding are omitted.

ordination arc" around M^+, thereby maximizing the space available to adjacent organic moieties.[2a] One particularly notable distinction exists between the cyclized ladder in the lithium complex of hexamethyleneimine, $[H_2C(CH_2)_5NLi]_6$ (SEDVEC),[20] and the Type 2 ladder in the analogous ammonium chloride $H_2C(CH_2)_5NH_2Cl$ (HEXAMC)[29] (Figure 14).

Several examples of infinite polymeric alkali metal amide ladders do exist, incorporating either Li^+ (e.g. $\{[PhCH_2N(H)Li]_2\cdot PhCH_2NH_2\}_\infty$ (NECQER),[30] $\{[PhCH_2N(H)Li]_2\cdot C_4H_8O\}_\infty$ (JUPHAD),[31]

$\{[H_2NCH_2CH_2N(H)Li]\}_\infty$ (PIXVIB)[32]) or Na^+ (e.g. $\{[(t\text{Bu})N(H)Na]_3\cdot(t\text{Bu})NH_2\}_\infty$ (NEXKOQ)[6]). In each of these cases, one of the substituents of the amido anion is H so that the steric constraints associated with ladder formation are relaxed to some degree. Nonetheless, the ladder conformations are clearly influenced by interactions between the R groups of the $R(H)N^-$ moieties. In PIXVIB, for example, the ladders undulate so that the bulk of each organic moiety lies always to the outside of the curvature of the ladder and only the H atoms are brought to the inside of the concave sections (Figure 15a). A similar arrangement

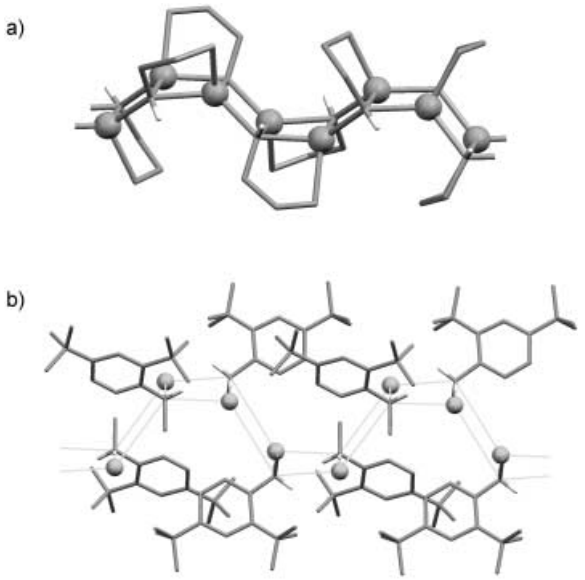

Figure 15. Undulating ladders in a) the lithium amide PIXVIB and b) the ammonium chloride CACVIM. Hydrogen atoms not involved in hydrogen bonding are omitted. Hydrogen atoms lie to the inside of the concave units in the inorganic ladder, while in the organic ladder methyl groups occupy these positions. A second NH_2 group on the amido moiety completes the coordination sphere of the Li^+ cations in PIXVIB.

is observed in NEXKOQ.[6] An analogous motif exists in the organic solid state in the form of the ammonium chloride CACVIM,[33] in which the N atom of the ammonium center bears one bulky 2,4-di(*t*Bu)-phenyl moiety and one methyl group and the methyl groups lie only to the inside of the concave units (Figure 15b). The tolerance for methyl groups in these positions compared with H atoms in the inorganic amide complexes again reflects the metric differences between the $N^+\cdots X^-$ and Li–N or Na–N contacts.

A note regarding organic iminium halides: Given that secondary ammonium halides display ring-stacking and ring-laddering behavior comparable to that shown by lithium amides, it might be expected that organic iminium halides ($R_2C{=}NH_2X$) would exhibit ring-stacking in the solid state. In fact, this is unlikely to be the case. Maps of the molecular electrostatic potential for simple iminium cations $[R_2C{=}NH_2]^+$ show that the C=N bond is generally polarized so that the most electropositive region lies on the C atom rather than the N atom.[34] Thus, the positive-charge center does not coincide with the hydrogen-bond center, and any association of $[R_2C{=}NH_2X]_n$ units is likely to occur through short $C^{\delta+}\cdots X^-$ rather than $N^{\delta+}\cdots X^-$ contacts. Few *simple* iminium halides have been examined crystallographically, but of ten structures identified in the CSD in which there is no interference from additional hydrogen-bond donors or acceptors, two form linear polymers (ACNITR20, JUPJAF) and eight form discrete dimers (CPXMAM, DULVIP, FACRUX, FAGNEG, KIJZAE, LEQHAQ, YATCAX, YITCEJ).[35] In one of the former cases (ACNITR20), the polymers are associated through short $C^{\delta+}\cdots X^-$ contacts (3.498 Å).

Conclusion

By considering in a general manner the geometrical characteristics of $N^+(-H)\cdots X^-$ contacts in secondary ammonium halides, R_2NH_2X (X = primarily Cl, Br), the ring-stacking and ring-laddering concepts of structural inorganic chemistry are shown to be applicable in the organic solid state. As for inorganic systems, association of $R_2NH_2^+X^-$ ion pairs is driven principally by electrostatic forces, increasing the coordination numbers of N^+ and X^-, thereby maximizing Coulombic energy. Each of the preferred directions of approach of X^- towards the N^+ center lies in the $H{-}N^+{-}H$ plane, so that association in a lateral manner is most common, forming in many cases extended ladder motifs. Several motifs based on stacking association are also observed. In general, the distribution of $N^+(-H)\cdots X^-$ distances in the organic systems mirrors that observed in alkali metal amide complexes, and may be considered to be derived from a balance between the directional preferences of $N^+{-}H\cdots X^-$ hydrogen bonds and the (primarily steric) constraints imposed by interactions between the R groups of the organic moieties. This correlates with existing notions in alkali metal amides of a balance between some degree of directional bonding from sp^3 hybrid atomic orbitals on R_2N^- and the steric constraints imposed by the R groups of the amido moiety. The analogy between inorganic metal-amide complexes, $[R_2NM]_n$, and secondary ammonium halides, R_2NH_2X, offers clear opportunities for systematic study of the effects of amide geometry on the structural motifs formed in both inorganic complexes and organic hydrogen-bonded systems. Just as the extensive organic sample provides insight into the motifs observed in alkali metal complexes, information derived from the inorganic complexes may be used to suggest new experiments in the organic solid state: obvious immediate targets are fragmented ladders based on secondary ammonium halides, incorporating some other hydrogen-bond donor molecule in the "Lewis base solvation" role. The metric differences between $N^+{-}H\cdots X^-$ hydrogen bonds and N–M interactions mean that *direct* comparisons may be few. Indeed, examples certainly exist in which direct structural correlation is not observed, for example, the cyclized ladder in the crystal structure of the lithium salt of hexamethyleneimine, $[H_2C(CH_2)_5NLi]_6$,[20] and the Type 2 ladder in $H_2C(CH_2)_5NH_2Cl$.[29] Differences such as these, however, and their relation to the metric differences between the N^+

−H···X⁻ and N−M interactions are likely to be of equal interest for elucidating further the factors governing the self-assembly of these systems.

Experimental Section

Database searches were performed with the November 2002 release of the Cambridge Structural Database (version 5.24, 272066 entries) using Conquest 1.5.[36] The data were analyzed using the MERCURY[36] and EXCEL packages.[37] To examine initially the N^+–H···X^- hydrogen-bond motifs in secondary organic ammonium halides, the search fragment C_2NH_2 was specified, together with two X (= F, Cl, Br, or I) defined as making no intramolecular bonds (i.e. discrete X^- anions). The positions of the terminal H atoms were normalized (1.03 Å), and two intermolecular H···X contacts in the range 1–4 Å were specified, together with associated N^+–H···X^- angles in the range 90–180°; these criteria reflect the directional characteristics of the hydrogen bond rather than any arbitrary distance cut-off. A search of only organic molecules provided 333 structures, comprising 3 fluoride, 267 chloride, 59 bromide, and 5 iodide complexes (1 structure KATXAE10 containing both fluoride and chloride). Duplicate entries were removed and the structures were examined manually to remove also those with more than one ammonium center and those in which other donors and acceptors participate in the hydrogen-bond network. For the latter purpose, structures were omitted in which the N^+–H bonds of the ammonium moiety formed hydrogen bonds to any atom other than X^-, as were those in which any other hydrogen-bond donor formed a hydrogen bond to X^-. Manual filtering was preferred to automated removal of structures with other short H···X contacts to ensure correct treatment of cases in which other hydrogen bonds are present but do not interfere with the N^+–H···X^- system. Following filtering, 148 chlorides, 16 bromides, and 2 iodides remained. For each of these structures, the local environment of N^+ was examined and the three shortest N^+···X^- vectors were retained, regardless of magnitude. Where more than three N^+···X^- vectors of comparable magnitude were present, all were retained. The coordinates of the relevant atoms were orthogonalized and the values of ϕ and θ were calculated within EXCEL. A full list of the 166 structures and associated ϕ and θ values is available as Supporting Information.

For the inorganic complexes, the CSD search was intended to locate ring-stacked and ring-laddered complexes only, for the purpose of comparison with the organic ammonium halide examples. To this end, the search fragment C_2N was specified (C–N bonds of any type), making at least *three* contacts (defined as either *intra-* or *inter*molecular) to M (= Li, Na) with N−M less than 3.0 Å. This search yielded 30 structures (24 Li, 5 Na, 1 Li/Na). The subset was filtered manually to remove structures in which three C atoms are bound to N (i.e. tertiary amides) and structures in which N is sp^2 hybridized. In cases where several different amide moieties were present, structures were retained where they contained one suitable secondary amide moiety, and only those suitable N centers were considered subsequently. For the 58 amide moieties retained in 16 structures (12 Li, 2 Na, 2 Li/Na), the ϕ and θ parameters were calculated for all bonded N−M contacts. A full list is available as Supporting Information. In each case, the distinction between "bonded" and "non-bonded" N−M contacts was quite clear, the non-bonded contacts being at least 1 Å longer than the bonded contacts. For the purposes of the statistical analysis, amide moieties bearing one H atom (i.e. $R(H)N^-$) were not included, since the uncertainty associated with the position of the H atom leads to significant uncertainty in the definition of ϕ and θ.

Acknowledgements

This work was supported by the Carlsbergfondet, Denmark. I am grateful to Dr. Frank Jensen (University of Southern Denmark) for calculation of molecular electrostatic potential maps for the model ammonium and iminium cations and to Dr. Dominic S. Wright (University of Cambridge, UK) for arousing my interest in this topic.

[1] a) D. Barr, W. Clegg, R. E. Mulvey, R. Snaith, K. Wade, *J. Chem. Soc. Chem. Commun.* **1986**, 295; b) D. R. Armstrong, D. Barr, W. Clegg, R. E. Mulvey, D. Reed, R. Snaith, K. Wade, *J. Chem. Soc. Chem. Commun.* **1986**, 869.

[2] Review articles: a) K. Gregory, P. von R. Schleyer, R. Snaith, *Adv. Inorg. Chem.* **1991**, *37*, 47; b) R. E. Mulvey, *Chem. Soc. Rev.* **1991**, *20*, 167; c) R. E. Mulvey, *Chem. Soc. Rev.* **1998**, *27*, 339; d) A. Downard, T. Chivers, *Eur. J. Inorg. Chem.* **2001**, 2193.

[3] P. B. Hitchcock, M. F. Lappert, W.-P. Leung, D.-S. Liu, T. C. W. Mak, Z.-X. Wang, *J. Chem. Soc. Dalton Trans.* **1999**, 1263 (CSD refcode: LAJQAO).

[4] D. R. Armstrong, D. Barr, R. Snaith, W. Clegg, R. E. Mulvey, K. Wade, D. Reed, *J. Chem. Soc. Dalton Trans.* **1987**, 1071 (DIFGUU10).

[5] D. Armstrong, D. Barr, W. Clegg, S. M. Hodgson, R. E. Mulvey, D. Reed, R. Snaith, D. S. Wright, *J. Am. Chem. Soc.* **1989**, *111*, 4719 (KARTOM).

[6] W. Clegg, K. W. Henderson, L. Horsburgh, F. M. Mackenzie, R. E. Mulvey, *Chem. Eur. J.* **1998**, *4*, 53 (NEXKOQ).

[7] D. K. Kennepohl, S. Brooker, G. M. Sheldrick, H. W. Roesky, *Chem. Ber.* **1991**, *124*, 2223 (SOLXUM).

[8] D. Barr, W. Clegg, R. E. Mulvey, R. Snaith, *J. Chem. Soc. Chem. Commun.* **1984**, 285 (ZEGNII).

[9] G. R. Desiraju, *Angew. Chem.* **1995**, *107*, 2541; *Angew. Chem. Int. Ed. Engl.* **1995**, *34*, 2311.

[10] A. D. Bond, E. L. Doyle, *Chem. Commun.* **2003**, 2324.

[11] H. Chen, R. A. Bartlett, H. V. R. Dias, M. M. Olmstead, P. P. Power, *Inorg. Chem.* **1991**, *30*, 3390.

[12] F. H. Allen, *Acta Crystallogr. Sect. B* **2002**, *58*, 380; CSD Version 5.24, November 2002 (272066 entries), Cambridge Crystallographic Data Centre, 12 Union Road, Cambridge, CB2 1EZ, U.K.

[13] The number of structures containing secondary ammonium cations and fluoride anions is very small (only five were identified), and there are no examples in which the N^+–H···F^- hydrogen-bond motifs are not disrupted by additional hydrogen-bond interactions.

[14] B. Rees, R. Weiss, *Acta Crystallogr. Sect. B* **1971**, *27*, 932 (TMPIPO). The resemblance to the fourfold motif in the Li derivative of 2,2,6,6-tetramethylpiperidine is striking: M. F. Lappert, M. J. Slade, A. Singh, J. L. Atwood, R. D. Rogers, R. Shakir, *J. Am. Chem. Soc.* **1983**, *105*, 302 (BUXNUD).

[15] R. E. Rosenfield Jr. , R. Parthasarathy, J. D. Dunitz, *J. Am. Chem. Soc.* **1977**, *99*, 4860.

[16] a) H. A. Karapetyan, Y. T. Struchkov, G. G. Dvoryantseva, *Cryst. Struct. Commun.* **1982**, *11*, 1441 (BORXUB); b) M. Bukowska-Stzyzewska, W. Dubrowolska, J. Skoweranda, T. Gajda, A. Zwierzak, *J. Mol. Struct.* **1980**, *69*, 117 (BRPYRL); c) W. C. Stallings, C. T. Monti, J. P. Glusker, *Acta Crystallogr. Sect. B* **1982**, *38*, 177 (CETEAN10); d) M. Yokota, H. Uekusa, Y. Ohashi, *Bull. Chem. Soc. Jpn.* **1999**, *72*, 1731 (HOTZOF); e) D. Mondeshka, I. Angelova, B. Stensland, P.-E. Werner, C. Ivanov, *Acta Chem. Scand.* **1992**, *46*, 54 (PEFCUY); f) J. Ouhabi, M. Saux, A. Carpy, *Acta Crystallogr. Sect. C* **1990**, *46*, 2160 (SIFGUJ); g) T. M. Georgiadis, M. M. Georgiadis, F. Diederich, *J. Org. Chem.* **1991**, *56*, 3362 (SOBFIY); h) H.-G. Klebe, V. G. Krishnan, A. Weiss, H. Fueß, *Eur. Cryst. Meeting* **1983**, *8*, 245 (TAJRUR); i) Z. Jia, J. W. Quail, V. K. Arora, J. R. Dimmock, *Acta Crystallogr. Sect. C* **1988**, *44*, 2114 (VABFIN); j) M. Dobler, J. D. Dunitz, *Helv. Chim. Acta* **1964**, *47*, 695 (AZNONB); k) K. Frydenvang, L. M. Hansen, B. Jensen, *Acta Crystallogr. Sect. C* **1995**, *51*, 2053 (ZENJAD).

[17] Averages derived from 352 fragments in 314 structures for the chlorides and 104 fragments in 96 structures for the bromides. See Supporting Information.

[18] T. Steiner, *Angew. Chem.* **2002**, *114*, 50; *Angew. Chem. Int. Ed.* **2002**, *41*, 48.

[19] a) G. Boche, I. Langlotz, M. Marsch, K. Harms, N. E. S. Nudelman, *Angew. Chem.* **1992**, *104*, 1239; *Angew. Chem. Int. Ed. Engl.* **1992**, *31*, 1205 (KUPSET); b) K. W. Henderson, P. G. Williard, *Organometallics* **1999**, *18*, 5620 (XEWFIO).

[20] This leads to interchange of the second and third longest contacts in the scatterplot of Figure 2a compared with the other structures. The distribution of contacts in CETEAN10 is comparable to that in the

"cyclized ladder" in the crystal structure of the lithium salt of hexamethyleneimine, $[H_2C(CH_2)_5NLi]_6$: R. Snaith, D. Barr, D. S. Wright, W. Clegg, S. M. Hodgson, G. R. Lamming, A. J. Scott, R. E. Mulvey, *Angew. Chem.* **1989**, *101*, 1279; *Angew. Chem. Int. Ed. Engl.* **1989**, *28*, 1241 (SEDVEC).

[21] a) J.-M. Leger, J.-C. Colleter, A. Carpy, *Cryst. Struct. Commun.* **1982**, *11*, 1363 (BOTPAB); b) M. Mayer, G. Perez, M. N. Petit, G. Coquerel, *Cryst. Struct. Commun.* **1982**, *11*, 1853 (BUHCIQ); c) L. F. Groux, F. Belanger-Gariepy, D. Zargarian, *Acta Crystallogr. Sect. C* **1999**, *55*, IUCR9900130 (CARQIV); d) C. van der Brempt, F. Durant, G. Evrard, *Bull. Soc. Chim. Belg.* **1986**, *95*, 139 (DIZVUD); e) H.-K. Fun, K. Chinnakali, I. A. Razak, S.-Z. Zhan, C.-J. Hu, Q. Meng, *Acta Crystallogr. Sect. C* **1999**, *55*, 766 (HIYDOI); f) G. R. Girard, W. E. Bondinell, L. M. Hillegass, K. G. Holden, R. G. Pendleton, I. Uzinskas, *J. Med. Chem.* **1989**, *32*, 1566 (JARSAW); g) V. Kettman, F. Pavelcik, J. Majer, A. Rybar, *Acta Crystallogr. Sect. C* **1989**, *45*, 282 (KADNIM); h) E. Vazquez, A. Galindo, D. Gnecco, S. Berenes, J. L. Teran, R. G. Enriquez, *Tetrahedron: Asymmetry* **2001**, *12*, 3209 (MIXTAO); i) Y. Ishihara, T. Tanaka, W. Miwatashi, A. Fujishima, G. Goto, *J. Chem. Soc. Perkin Trans. 1* **1994**, 2993 (POJVOZ, POJVUF); j) R. J. Hausin, P. W. Codding, *J. Med. Chem.* **1991**, *34*, 511 (SIWCAC); k) J. A. Suchocki, E. L. May, T. J. Martin, C. George, B. R. Martin, *J. Med. Chem.* **1991**, *34*, 1003 (VIPNIR); l) M. Froimowitz, K.-M. Wu, C. George, A. VanderVeer, Q. Shi, H. M. Deutsch, *Struct. Chem.* **1998**, *9*, 295 (WOGPOX); m) J. Buchler, C. Maichle-Mossmer, K.-A. Kovar, *Z. Naturforsch. B* **2000**, *55*, 1124 (WOWXIP, WOWXUB); n) K. Ramig, L. Brockunier, P. W. Rafalko, L. A. Rozov, *Angew. Chem.* **1995**, *107*, 254; *Angew. Chem. Int. Ed. Engl.* **1995**, *34*, 222 (YIJFOM).

[22] a) M. Plamo, M. Klinga, M. Leskela, *Z. Kristallogr.* **1997**, *212*, 200 (GEQWUU); b) C. L. Klein, T. A. Banks, D. Rouselle, *Acta Crystallogr. Sect. C* **1991**, *47*, 1478 (JINGIW); c) D. Carlstrom, *Acta Crystallogr. Sect. B* **1976**, *32*, 2460 (MAESCI); d) P. G. Jones, A. K. Fischer, H. Vogt, *Z. Kristallogr.* **1994**, *209*, 834 (POSTUM); e) J. Karolak-Wojciechowska, W. Kwiatkowski, S. W. Markowicz, *J. Crystallogr. Spectrosc. Res.* **1989**, *19*, 893 (SEFWAB); f) A. Fischer, I. Neda, P. G. Jones, R. Schmutzler, *Phosphorus Sulfur Silicon Relat. Elem.* **1994**, *91*, 103 (YUWWIW).

[23] The notation is that of Wells: n^p describes p polygons of n edges meeting at each vertex of the two-dimensional net. In the commonly used "vertex symbol" notation, the 4^4 net would be denoted [4.4.4.4]. The 4.8^2 net referred to subsequently would be [4.8.8]: see M. O'Keeffe, M. Eddaoudi, H. Li, T. Reineke, O. M. Yaghi, *J. Solid State Chem.* **2000**, *152*, 3.

[24] N. D. R. Barnett, R. E. Mulvey, W. Clegg, P. A. O'Neil, *J. Am. Chem. Soc.* **1991**, *113*, 8187 (KOGYUA).

[25] S. C. Nyburg, *Acta Crystallogr. Sect. C* **1996**, *52*, 192 (ZIVMUM).

[26] J. Weinstock, H.-J. Oh, C. W. De Brosse, D. S. Eggleston, M. Wise, K. E. Flaim, G. W. Gessner, J. L. Sawyer, C. Kaiser, *J. Med. Chem.* **1987**, *30*, 1303 (DUTKAE10).

[27] M. G. Gardiner, C. L. Raston, *Inorg. Chem.* **1996**, *35*, 4047 (TETGOO).

[28] Ammonium moieties bearing more than one N^+ center were excluded from the far more extensive organic sample.

[29] T. S. Cameron, H. W. Scheeren, *J. Chem. Soc. Chem. Commun.* **1977**, 939 (HEXAMC).

[30] A. R. Kennedy, R. E. Mulvey, A. Robertson, *Chem. Commun.* **1998**, 89 (NECQER).

[31] W. Clegg, S. T. Liddle, R. E. Mulvey, A. Robertson, *Chem. Commun.* **1999**, 511 (JUPHAD).

[32] G. R. Kowach, C. J. Warren, R. C. Haushalter, F. J. Di Salvo, *Inorg. Chem.* **1998**, *37*, 156 (PIXVIB).

[33] F. Riviere, S. Ito, M. Yoshifuji, *Tetrahedron Lett.* **2002**, *43*, 119 (CACVIM).

[34] Molecular electrostatic potential maps calculated for the model species $[Me_2C{=}NH_2]^+$ (Gaussian-98, B3LYP/6-31G**) confirm that the most electropositive region in the iminium cation is located in the vicinity of the C atom rather than the N atom.

[35] a) J. M. Williams, S. W. Peterson, G. M. Brown, *Inorg. Chem.* **1968**, *7*, 2577 (ACNITR20); b) K. Peters, E.-M. Peters, B. Ventzke, A. Hetzheim, *Z. Kristallogr.* **1999**, *214*, 169 (JUPJAF); c) J. Galloy, J.-P. Putzeys, G. Germain, J. P. Declercq, M. van Meerssche, *Acta Crystallogr. Sect. B* **1974**, *30*, 2460 (CPXMAM); d) C. van der Brempt, G. Evrard, F. Durant, *Acta Crystallogr. Sect. C* **1986**, *42*, 1206 (DULVIP); e) A. K. Fischer, P. G. Jones, *Acta Crystallogr. Sect. E* **2002**, *58*, o218 (FACRUX); f) K. Peters, E.-M. Peters, K. Grunwald, A. Hetzheim, *Z. Kristallogr.* **1998**, *213*, 761 (FAGNEG); g) C. Boga, L. Forlani, C. Silvestroni, A. Bonamartini Corradi, P. Sgarabotto, *J. Chem. Soc. Perkin Trans. 1*, **1999**, 1363 (KIJZAE); h) B. Pniewska, A. Rykowski, W. Pucko, *Pol. J. Chem.* **1997**, *71*, 1102 (LEQHAQ); i) W. P. Fehlhammer, F. Schoder, G. Beck, S. Schrolkamp, *Z. Anorg. Allg. Chem.* **1993**, *619*, 1171 (YATCAX); j) N. A. Martem'yanova, Y. M. Chunaev, N. M. Przhiyalgovskaya, L. N. Kurkovskaya, O. S. Filipenko, S. M. Aldoshin, *Khim. Geterotsikl. Soedin.* **1993**, 415 (YITCEJ).

[36] I. J. Bruno, J. C. Cole, P. R. Edgington, M. Kessler, C. F. Macrae, P. McCabe, J. Pearson, R. Taylor, *Acta Crystallogr. Sect. B* **2002**, *58*, 389.

[37] Microsoft Corporation, EXCEL-97, **1997**.

Received: November 7, 2003 [F5700]